AD-A053 898 HARRY DIAMOND LABS ADELPHI MD F/G 20/14
ELECTROMAGNETIC WAVES IN ANISOTROPIC DIELECTRIC SLABS.(U)
APR 78 N KARAYIANIS
UNCLASSIFIED HDL-TR-1845 NL

1 OF 1
AD A
053898

END
DATE FILMED
6-78
DDC

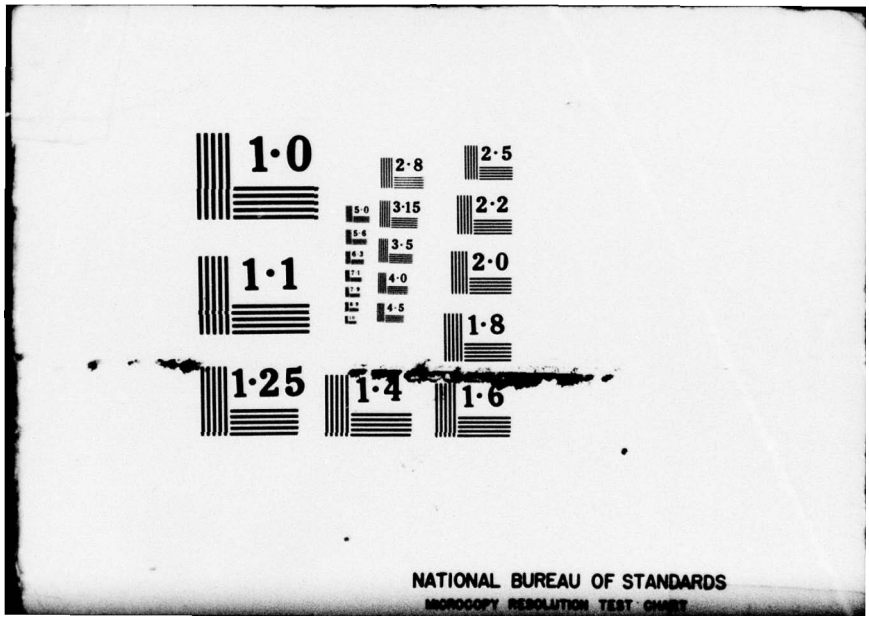
1·0
1·1
1·25
1·4
1·6
1·8
2·0
2·2
2·5
2·8
3·15
3·5
4·0
4·5
NATIONAL BUREAU OF STANDARDS
MICROCOPY RESOLUTION TEST CHART

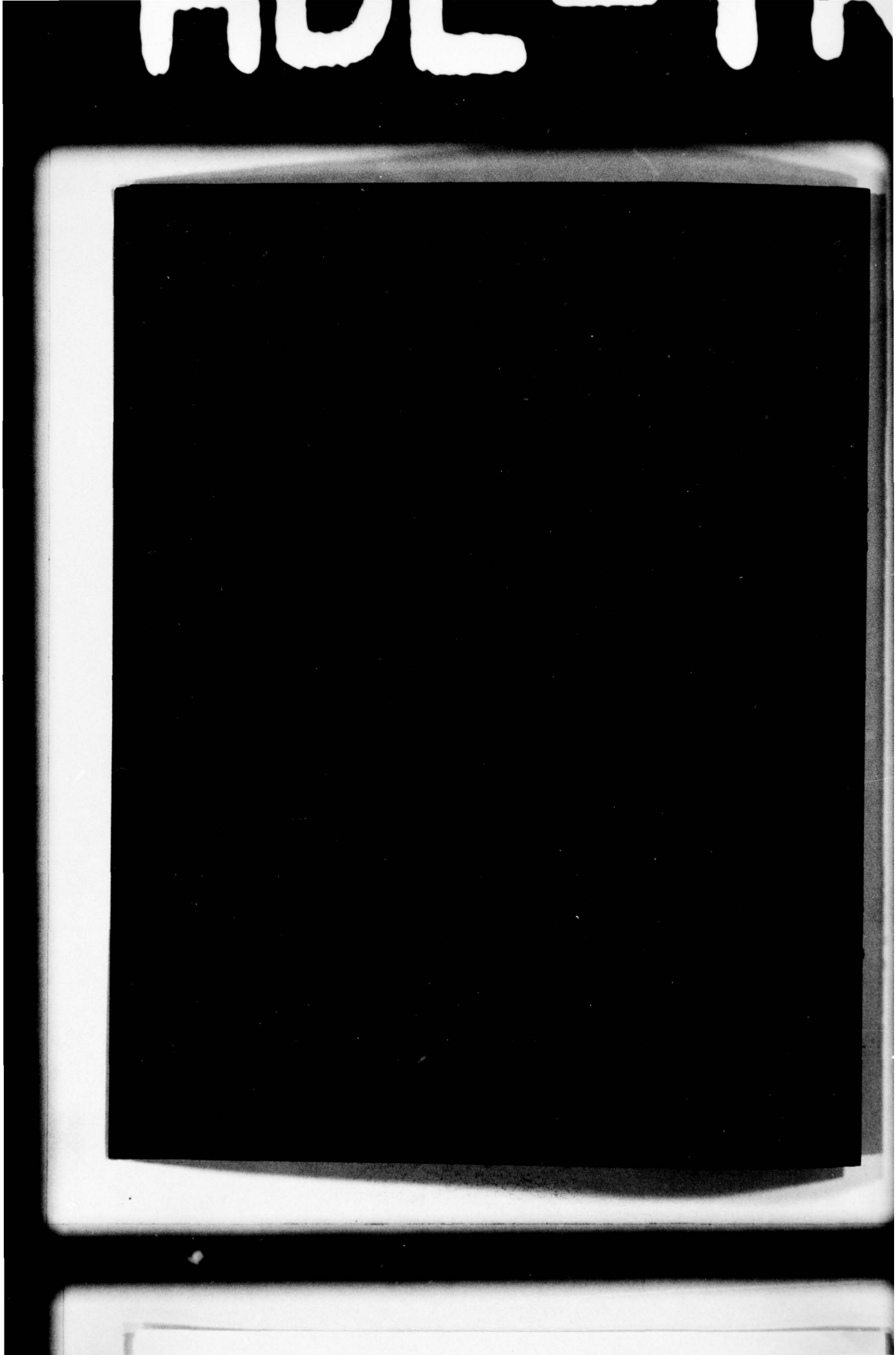

UNCLASSIFIED

SECURITY CLASSIFICATION OF THIS PAGE (When Data Entered)

REPORT DOCUMENTATION PAGE

READ INSTRUCTIONS BEFORE COMPLETING FORM

1. REPORT NUMBER: HDL-TR-1845
2. GOVT ACCESSION NO.
3. RECIPIENT'S CATALOG NUMBER
4. TITLE (and Subtitle): Electromagnetic Waves in Anisotropic Dielectric Slabs
5. TYPE OF REPORT & PERIOD COVERED: Technical Report
6. PERFORMING ORG. REPORT NUMBER
7. AUTHOR(s): Nick Karayianis
8. CONTRACT OR GRANT NUMBER(s): PRON: A17R000101A1A9; DA: 1T161101A91A
9. PERFORMING ORGANIZATION NAME AND ADDRESS: Harry Diamond Laboratories, 2800 Powder Mill Road, Adelphi, MD 20783
10. PROGRAM ELEMENT, PROJECT, TASK AREA & WORK UNIT NUMBERS: Program Ele: 6.11.01.A
11. CONTROLLING OFFICE NAME AND ADDRESS: U. S. Army Materiel Development and Readiness Command, Alexandria, VA 22333
12. REPORT DATE: Apr[illegible]78
13. NUMBER OF PAGES: 26 (25 pp.)
14. MONITORING AGENCY NAME & ADDRESS (if different from Controlling Office)
15. SECURITY CLASS. (of this report): UNCLASSIFIED
15a. DECLASSIFICATION/DOWNGRADING SCHEDULE

16. DISTRIBUTION STATEMENT (of this Report)

Approved for public release; distribution unlimited.

17. DISTRIBUTION STATEMENT (of the abstract entered in Block 20, if different from Report)

P.E 611101A LPN-HDL-A10735

18. SUPPLEMENTARY NOTES

HDL Project: A10735
DRCMS Code: 611101.91.A0011

19. KEY WORDS (Continue on reverse side if necessary and identify by block number)

Anisotropic media
Lithium niobate
Electromagnetic waves
Dielectric slabs

20. ABSTRACT (Continue on reverse side if necessary and identify by block number)

The theory of electromagnetic wave modes in an infinite anisotropic dielectric slab is reviewed. The theory is specialized to lithium niobate cut with its z-axis in the plane of the slab. It is shown that pure transverse electric (TE) and transverse magnetic (TM) modes propagate along the principal axes of the dielectric, but that coupled TE- and TM-like modes result for propagation at small angles with respect to these axes. The lowest order modes--the fundamental TE(0) and TM(0)

DD FORM 1 JAN 73 1473 EDITION OF 1 NOV 65 IS OBSOLETE

UNCLASSIFIED

SECURITY CLASSIFICATION OF THIS PAGE (When Data Entered)

163 050

modes--are determined, and the associated fields are plotted. One higher order mode--the $TM_0^{(2)}$-like mode propagating at an angle of 19 deg with respect to one of the principal axes--also is plotted. These results relate to the problem of the interaction of sheet laser beams with surface acoustic waves.

CONTENTS

FIGURES

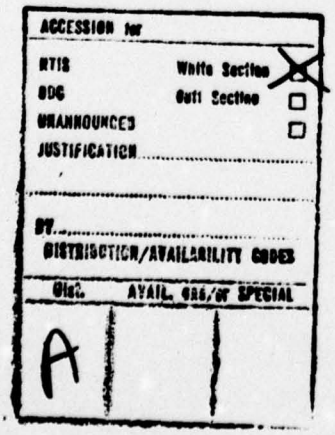

1. INTRODUCTION

In surface acoustic wave (SAW) devices, the interaction between laser beams and acoustic waves must be understood by considering the allowed surface modes of both disturbances. In this report, the formalism for determining the modes for electromagnetic (laser) waves is reviewed and solved for propagation in an anisotropic dielectric slab. It is shown that pure transverse electric (TE) and transverse magnetic (TM) modes are possible only if propagation occurs parallel to the principal axes of the material, but that coupled TE- and TM-like modes occur for propagation at small angles with respect to these axes.

In section 2, the formalism is given for determining the modes for propagation at an angle with respect to one principal axis (y') of the material and parallel to another (x').

In section 3, results are obtained specifically for 0.53-μm radiation (doubled 1.06-μm radiation from a neodymium:yttrium aluminum garnet (Nd:YAG) laser) in lithium niobate ($LiNbO_3$). There, TE- and TM-like modes are obtained for various thicknesses of a slab backed on one face by a perfect conductor and on the other by free space. For some typical examples, the Poynting vector, S_y, indicating the magnitude of power flow, is plotted versus distance into the slab from the surface to indicate the concentration of the power. It is expected that these data when correlated with similar calculations for the SAW's will determine more precisely the regions where the interaction is strongest. These results will help clarify the dependence of the observed phenomena on polarization and the angle of propagation. Computer programs have been written to perform these calculations for the general case.

2. THEORY

In the cgs system of units, Maxwell's equations in the *absence of sources* are

$$\nabla \times E = -\frac{1}{c}\frac{\partial B}{\partial t} \quad , \tag{1a}$$

$$\nabla \times H = \frac{1}{c}\frac{\partial D}{\partial t} \quad , \tag{1b}$$

where

$$B = \mu H \quad , \tag{2a}$$

$$D = \varepsilon E \quad , \tag{2b}$$

and μ, the permeability, and ε, the dielectric constant, may be tensors. Considering the quantities E, B, H, and D as column vectors, ∇X, μ, and ε as tensors, and $\nabla\cdot$ as a row vector, we have, for example,

$$\nabla\cdot = \left(\frac{\partial}{\partial x} \quad \frac{\partial}{\partial y} \quad \frac{\partial}{\partial z}\right) \tag{3}$$

and

$$\nabla X = \begin{bmatrix} 0 & -\frac{\partial}{\partial z} & \frac{\partial}{\partial y} \\ \frac{\partial}{\partial z} & 0 & -\frac{\partial}{\partial x} \\ -\frac{\partial}{\partial y} & \frac{\partial}{\partial x} & 0 \end{bmatrix} \tag{4}$$

Thus, one may easily see that the product of $\nabla\cdot$ and ∇X gives

$$\nabla\cdot(\nabla X) = \left(d^2_{yz} \quad d^2_{zx} \quad d^2_{xy}\right) , \tag{5}$$

where

$$d^2_{yz} = \frac{\partial^2}{\partial y\, \partial z} - \frac{\partial^2}{\partial z\, \partial y} \tag{6}$$

and similarly for d^2_{zx} and d^2_{xy}. Assuming that the functions (column vectors) that are to be operated on by $\nabla\cdot(\nabla X)$ are well behaved, the partial derivatives may be interchanged and

$$\nabla\cdot(\nabla X) = 0 . \tag{7}$$

Operating with $\nabla\cdot$ on equations (1a) and (1b), one obtains

$$\nabla\cdot B = \nabla\cdot D = 0 \tag{8}$$

as a natural consequence of Maxwell's equations with no sources.

To solve Maxwell's equations as a superposition of plane waves of the form

$$\exp(ik\cdot r - i\omega t) , \tag{9}$$

equations (1a) and (1b) become

$$kXE = k_o \mu H, \tag{10a}$$

$$kXH = -k_o \varepsilon E, \tag{10b}$$

where

$$k_o = \omega/c \ , \tag{11}$$

ω is the angular frequency, and c is the velocity of light.

The most general equation for E becomes

$$UE = 0, \tag{12}$$

where

$$U = (kX)\mu^{-1}(kX) + k_o^2 \varepsilon \ . \tag{13}$$

Analogous to equation (4),

$$kX = \begin{bmatrix} 0 & -k_z & k_y \\ k_z & 0 & -k_x \\ -k_y & k_x & 0 \end{bmatrix} \ . \tag{14}$$

Since equation (12) represents a set of three homogeneous equations in the E_x, E_y, and E_z components of E, solutions are obtained when the determinant of coefficients vanishes,

$$\det(U) = 0 \ . \tag{15}$$

In this report, we consider only the case where μ is a scalar and equation (15) becomes (multiplying through by μ)

$$\det\left[(kX)(kX) + k_o^2 \mu\varepsilon\right] = 0 \ , \tag{16}$$

where from equation (14) one obtains

$$(kX)(kX) = \begin{bmatrix} -\left(k_y^2 + k_z^2\right) & k_x k_y & k_z k_x \\ k_x k_y & -\left(k_z^2 + k_x^2\right) & k_y k_z \\ k_z k_x & k_y k_z & -\left(k_x^2 + k_y^2\right) \end{bmatrix} \ . \tag{17}$$

The determinant given by equation (16) gives relationships among the components k_x, k_y, and k_z of k and ω (through k_o) in the medium, and any boundary conditions will further limit their allowed values. Once values for the components of k are known, then all the components of E and H may be solved in terms of any one of them by equations (1a) and (1b).

Taking the tensor components of ε to be ε_{ij}, where $\varepsilon_{ij} = \varepsilon_{ji}$, then equation (16) gives

$$\left[-\left(k_y^2 + k_z^2\right) + k_o^2\,\mu\varepsilon_{11}\right]\left[-\left(k_z^2 + k_x^2\right) + k_o^2\,\mu\varepsilon_{22}\right]\left[-\left(k_x^2 + k_y^2\right) + k_o^2\,\mu\varepsilon_{33}\right]$$
$$-\left[-\left(k_y^2 + k_z^2\right) + k_o^2\,\mu\varepsilon_{11}\right]\left[k_y k_z + k_o^2\,\mu\varepsilon_{23}\right]^2$$
$$-\left[-\left(k_z^2 + k_x^2\right) + k_o^2\,\mu\varepsilon_{22}\right]\left[k_z k_x + k_o^2\,\mu\varepsilon_{13}\right]^2$$
$$-\left[-\left(k_x^2 + k_y^2\right) + k_o^2\,\mu\varepsilon_{33}\right]\left[k_x k_y + k_o^2\,\mu\varepsilon_{12}\right]^2$$
$$+2\left[k_y k_z + k_o^2\,\mu\varepsilon_{23}\right]\left[k_z k_x + k_o^2\,\mu\varepsilon_{13}\right]\left[k_x k_y + k_o^2\,\mu\varepsilon_{12}\right] = 0\ . \qquad (18)$$

This equation gives the most general relationship between the components of k under the assumptions of an exponential space-time variation given by equation (9) and of scalar permeability μ.

We further limit the considerations in this report to no propagation in the z direction ($k_z = 0$), and $\varepsilon_{12} = \varepsilon_{13} = 0$.

Equation (18), where $k_z = \varepsilon_{12} = \varepsilon_{13} = 0$, reduces to

$$\left[-k_x^2 + k_E^2\right]\left[-k_x^2 + k_M^2\right] = k_{23}^4\ , \qquad (19)$$

where

$$k_E^2 = -k_y^2 + k_o^2\,\mu\varepsilon_{33} \quad \text{(TE mode)}, \qquad (20a)$$

$$k_M^2 = \frac{\varepsilon_{22}}{\varepsilon_{11}}\left(-k_y^2 + k_o^2\,\mu\varepsilon_{11}\right) \quad \text{(TM mode)}, \qquad (20b)$$

$$k_{23}^4 = k_o^2\,\mu\,\frac{\varepsilon_{23}^2}{\varepsilon_{11}}\left(-k_y^2 + k_o^2\mu\varepsilon_{11}\right) = \frac{k_o^2\mu\varepsilon_{23}^2}{\varepsilon_{22}}\,k_M^2\ . \qquad (20c)$$

The TE and TM modes exist in the limit of vanishing ε_{23} (resulting in a diagonal dielectric tensor). The TE mode for diagonal ε is a solution where $E_x = E_y = 0$; hence, $E = E_z$, which is transverse to the direction of propagation and experiences only the ε_{33} dielectric constant as shown in equation (20a). The TM mode for diagonal ε is a solution where $H_x = H_y = 0$; hence, $H = H_z$, but E lies only in the x-y plane and therefore experiences the combination of ε_{11} and ε_{22} dielectric constants shown in equation (20b).

When $\varepsilon_{23} \neq 0$, as is considered below, these two modes are coupled as shown in equation (19). The specific problem that we solve is a bound wave propagating parallel to the surface of an infinite dielectric slab surfaced with a perfect conductor on one face as shown in figure 1.

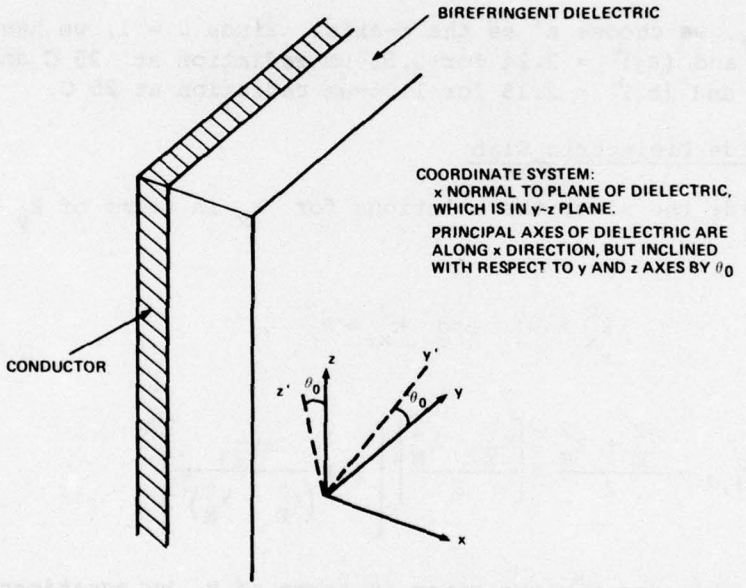

Figure 1. Representation of system to be solved for bound electromagnetic radiation propagating in x-y plane; boundaries only in x direction are considered, with slab being infinite in both y and z directions.

If the principal axes of the dielectric are parallel to the x-axis but rotated about x through an angle θ_0 as shown in figure 1, then we have

$$\varepsilon_{11} = \varepsilon_1 \ , \tag{21a}$$

$$\varepsilon_{22} = \varepsilon_2 \cos^2 \theta_0 + \varepsilon_3 \sin^2 \theta_0 \ , \tag{21b}$$

$$\varepsilon_{33} = \varepsilon_3 \cos^2 \theta_0 + \varepsilon_2 \sin^2 \theta_0 \ , \tag{21c}$$

$$\varepsilon_{23} = \left(\varepsilon_2 - \varepsilon_3\right) \cos \theta_0 \sin \theta_0 \ , \tag{21d}$$

where ε_1 , ε_2 , and ε_3 are the principal dielectric constants of the material. Alternatively, we may consider $-\theta_0$ as the angle at which the electromagnetic wave is launched with respect to the ε_2 principal axis of the material.

In $LiNbO_3$, we choose z' as the c-axis. Since $\mu = 1$, we have $(\varepsilon_1)^{\frac{1}{2}} = (\varepsilon_2)^{\frac{1}{2}} = 2.34$ and $(\varepsilon_3)^{\frac{1}{2}} = 2.24$ for 0.53-μm radiation at 25 C and $(\varepsilon_1)^{\frac{1}{2}} = (\varepsilon_2)^{\frac{1}{2}} = 2.24$ and $(\varepsilon_3)^{\frac{1}{2}} = 2.15$ for 1.06-μm radiation at 25 C.

2.1 Inside Dielectric Slab

Inside the slab, the solutions for k_x in terms of k_y are, from equation (19),

$$k_x^2 = k_1^2 \quad \text{and} \quad k_x^2 = k_2^2 \ , \tag{22a}$$

where

$$k_{1,2}^2 = \frac{k_E^2 + k_M^2}{2} \pm \left[\frac{k_E^2 - k_M^2}{2}\right] \left[1 + \frac{4k_{23}^4}{\left(k_E^2 - k_M^2\right)^2}\right]^{\frac{1}{2}} \tag{22b}$$

and where k_E^2, k_M^2, and k_{23}^4 are given in terms of k_y by equations (20a, b, c), respectively. From equations (1a) and (1b), one has

$$\frac{\partial}{\partial y} E_z = ik_o \mu H_x \ , \tag{23a}$$

$$-\frac{\partial}{\partial x} E_z = ik_o \mu H_y \ , \tag{23b}$$

$$\frac{\partial}{\partial x} E_y - \frac{\partial}{\partial y} E_x = ik_o \mu H_z \ , \tag{23c}$$

$$\frac{\partial}{\partial y} H_z = -ik_o \varepsilon_{11} E_x \quad , \tag{23d}$$

$$-\frac{\partial}{\partial x} H_z = -ik_o \left(\varepsilon_{22} E_y + \varepsilon_{23} E_z\right) \quad , \tag{23e}$$

$$\frac{\partial}{\partial x} H_y - \frac{\partial}{\partial y} H_x = -ik_o \left(\varepsilon_{23} E_y + \varepsilon_{33} E_z\right) \quad . \tag{23f}$$

The arbitrary solution in the slab is a linear combination of sines and cosines of $k_1 x$ and $k_2 x$. For convenience, we define coefficients u_1, u_2, u_3, and u_4 such that

$$E_z = \left(u_1 + u_2 t_1\right) \cos k_1 x + \varepsilon_{23} \left(u_3 + u_4 t_2\right) \cos k_2 x \quad , \tag{24a}$$

where

$$t_{1,2} = \tan k_{1,2} x \Big/ k_{1,2} \quad . \tag{24b}$$

From equation (23a),

$$H_x = k_y E_z \Big/ \left(\mu k_o\right) \quad . \tag{24c}$$

From equation (23b), one has

$$H_y = -i \left[\left(u_1 t_1 k_1^2 - u_2\right) \cos k_1 x + \varepsilon_{23} \left(u_3 t_2 k_2^2 - u_2\right) \cos k_2 x\right] \Big/ \left(\mu k_o\right). \tag{24d}$$

From equation (23f), one has

$$E_y = \left[\frac{\left(k_1^2 - k_E^2\right)}{\varepsilon_{23}} \left(u_1 + u_2 t_1\right) \cos k_1 x + \left(k_2^2 - k_E^2\right)\left(u_3 + u_4 t_2\right) \cos k_2 x\right] \Big/ \left(\mu k_o^2\right) \quad . \tag{24e}$$

From equations (23c, d) and (24e),

$$H_z = i\epsilon_{22}\left[\frac{\left(k_1^2 - k_E^2\right)}{\epsilon_{23}}\left(u_1 t_1 k_1^2 - u_2\right)\cos k_1 x + \left(k_2^2 - k_E^2\right)\left(u_3 t_2 k_2^2 - u_4\right)\cos k_2 x\right] \Big/ \left(\mu k_o k_M^2\right) \quad . \tag{24f}$$

Finally, from equations (23d) and (24f),

$$E_x = -k_y H_z \Big/ \left(\epsilon_{11} k_o\right) \quad . \tag{24g}$$

Thus, equations (24a) to (24g) give the six components of E and H in terms of the arbitrary constants u_1, u_2, u_3, and u_4, which are to be determined by the boundary conditions up to a constant factor.

2.2 Outside Dielectric Slab

Outside the dielectric slab, we have, in addition to the previously assigned conditions, $\epsilon_{11} = \epsilon_{22} = \epsilon_{33} = \mu = 1$ and $\epsilon_{23} = 0$. From equations (20a, b, c), which apply since they are perfectly general, $k_{23}^4 = 0$; and the solutions of equation (19) split into the TE and TM modes, which give the same solution, that is,

$$k_x^2 = -k_y^2 + k_o^2 \quad . \tag{25}$$

We are interested in a bound wave, so we choose

$$k_x = i\Gamma \quad , \tag{26}$$

so that

$$\Gamma^2 = k_y^2 - k_o^2 \quad , \tag{27}$$

and we look for solutions for positive Γ. The choice of sign given by equation (26) gives x variations of the form

$$e^{-\Gamma x} \quad , \tag{28}$$

which die in the positive x direction as shown in figure 1 if Γ is positive.

The spatial solution outside the slab may be written for E_z as

$$E_z = -u_5 e^{-\Gamma x} e^{ik_y y} \quad . \tag{29a}$$

Following the procedure for solving the various equations starting from equation (23a), we have

$$H_x = \frac{k_y}{k_o} E_z \quad , \tag{29b}$$

$$H_y = -i \frac{\Gamma}{k_o} E_z \quad , \tag{29c}$$

$$E_y = \lim_{\epsilon_{23} \to 0} \frac{1}{k_o^2 \epsilon_{23}} \left(-k_o^2 + k_y^2 - \Gamma^2 \right) E_z \quad . \tag{29d}$$

But since Γ^2 is related to k_y^2 according to equation (27), one gets an indeterminant form for E_y Thus, we may define E_y better by choosing H_z to have the spatial variation

$$H_z = iu_6 e^{-\Gamma x} e^{ik_y y} \Big/ \left(\mu k_o \right) \quad , \tag{30a}$$

and we obtain from equations (23d, e)

$$E_x = - \frac{k_y}{k_o} H_z \quad , \tag{30b}$$

$$E_y = i \frac{\Gamma}{k_o} H_z \quad . \tag{30c}$$

These equations are independent of, but analogous to, equations (29a, b, c).

2.3 Matching Boundary Conditions

We set E tangential and H tangential to be continuous across the dielectric-air boundary at x = 0, and we set E tangential zero at the metal boundary at x = -L, where L is the dielectric slab thickness.

From equations (24a) and (29a), we set E_z continuous at x = 0 to get

$$u_1 + \varepsilon_{23} u_3 = -u_5 \ ; \tag{31a}$$

from equations (24d) and (29c), we set H_y continuous at x = 0 to get

$$u_2 + \varepsilon_{23} u_4 = \mu\Gamma u_5 \ ; \tag{31b}$$

from equations (24e) and (30a, c), we set E_y continuous at x = 0 to get

$$\left(k_1^2 - k_E^2\right) u_1 + \varepsilon_{23}\left(k_2^2 - k_E^2\right) u_3 = -\varepsilon_{23}\Gamma u_6 \ ; \tag{31c}$$

from equations (24f) and (30a), we set H_z continuous at x = 0 to get

$$\left(k_1^2 - k_E^2\right) u_2 + \varepsilon_{23}\left(k_2^2 - k_E^2\right) u_4 = -\frac{\varepsilon_{23}}{\varepsilon_{22}} k_M^2 \, u_6 \ ; \tag{31d}$$

from equation (24a), we set $E_z = 0$ at x = -L to get

$$u_1 \cos k_1 L - u_2 \frac{\sin k_1 L}{k_1} + \varepsilon_{23} u_3 \cos k_2 L - \varepsilon_{23} u_4 \frac{\sin k_2 L}{k_2} = 0 \ ; \tag{31e}$$

from equation (24e), we set $E_y = 0$ at x = -L to get

$$\left(k_1^2 - k_E^2\right)\left(u_1 \cos k_1 L - u_2 \frac{\sin k_1 L}{k_1}\right) + \varepsilon_{23}\left(k_2^2 - k_E^2\right)\left(u_3 \cos k_2 L - u_4 \frac{\sin k_2 L}{k_2}\right) = 0 \ . \tag{31f}$$

For a solution, the following determinant of the coefficients must vanish:

$$\begin{bmatrix} 1 & 1 & 0 & 1 & 0 \\ 0 & 1 & 0 & 1 & -\mu\Gamma & 0 \\ k_1^2 - k_E^2 & 0 & k_2^2 - k_E^2 & 0 & 0 & \Gamma \\ 0 & k_1^2 - k_E^2 & 0 & k_2^2 - k_E^2 & 0 & k_M^2/\varepsilon_{22} \\ \cos k_1 L & -\frac{\sin k_1 L}{k_1} & \cos k_2 L & -\frac{\sin k_2 L}{k_2} & 0 & 0 \\ \left(k_1^2 - k_E^2\right)\cos k_1 L & -\left(k_1^2 - k_E^2\right)\frac{\sin k_1 L}{k_1} & \left(k_2^2 - k_E^2\right)\cos k_2 L & -\left(k_2^2 - k_E^2\right)\frac{\sin k_2 L}{k_2} & 0 & 0 \end{bmatrix} = 0 \qquad (32)$$

From equations (20a, b, c), (22b), and (27), each of the quantities in the determinant is expressed in terms of k_y^2. Thus, the solution of equation (32) gives the allowed values for k_y^2.

In the limit $\varepsilon_{23} \to 0$ ($\theta_0 = 0$ for propagation perpendicular to the c-axis in $LiNbO_3$), equations (31a to f) split into two independent sets of three equations. In general,

$$\frac{k_1^2 - k_E^2}{\varepsilon_{23}} = -\varepsilon_{23}\,\frac{\mu k_o^2 k_M^2}{\varepsilon_{22}\left(k_2^2 - k_E^2\right)} \qquad (33)$$

so that, in the limit $\varepsilon_{23} \to 0$,

$$k_1 \to k_E \ , \qquad (34a)$$

$$k_2 \to k_M \ , \qquad (34b)$$

$$\frac{k_1^2 - k_E^2}{\varepsilon_{23}} \to 0. \qquad (34c)$$

One solution is the TE solution obtained by striking columns 3, 4, and 6 in equation (32) and thereby getting

$$\begin{bmatrix} 1 & 0 & 1 \\ 0 & k_E & -\mu\Gamma \\ \cos k_E L & -\sin k_E L & 0 \end{bmatrix} = 0 \qquad (35)$$

or

$$1 + \frac{\mu\Gamma}{k_E} \tan k_E L = 0 \quad , \qquad (36)$$

with

$$k_E^2 = k_o^2 \mu\varepsilon_{33} - k_y^2 \quad ,$$
$$\Gamma^2 = k_y^2 - k_o^2 \quad .$$

The second solution is the TM solution obtained by striking columns 1, 2, and 5 in equation (32) and thereby getting

$$\begin{bmatrix} 1 & 0 & \Gamma \\ 0 & 1 & k_M/\varepsilon_{22} \\ \cos k_M L & -\sin k_M L & 0 \end{bmatrix} = 0 \qquad (37)$$

or

$$\tan k_M L - \frac{\Gamma\varepsilon_{22}}{k_M} = 0 \quad , \qquad (38)$$

with

$$k_M^2 = k_o^2 \mu\varepsilon_{22} - k_y^2 \varepsilon_{22}/\varepsilon_{11} \quad . \qquad (39)$$

The general solutions for equation (32) are given by

$$\left(k_2^2 - k_E^2\right)\left(1 + \mu\Gamma \frac{\tan k_1 L}{k_1}\right)\left(\frac{k_M^2}{\Gamma\varepsilon_{22}} \frac{\tan k_2 L}{k_2} - 1\right)$$

$$- \left(k_1^2 - k_E^2\right)\left(1 + \mu\Gamma \frac{\tan k_2 L}{k_2}\right)\left(\frac{k_M^2}{\Gamma\varepsilon_{22}} \frac{\tan k_1 L}{k_1} - 1\right) = 0 \quad . \qquad (40)$$

The second term vanishes as $\varepsilon_{23} \to 0$, since $k_1^2 \to k_E^2$, and the second and third factors in the first term give, respectively, the TE and TM solutions given by equations (36) and (38) ($k_2 \to k_M$ in this limit).

2.4 Transverse Electric-like Modes

We consider cases for which θ_0 is small so that from equation (21d) $\varepsilon_{23} << 1$. Thus, we refer to TE-like modes as those solutions of equation (40) where

$$\mu\Gamma \frac{\tan k_1 L}{k_1} \sim -1 \quad . \qquad (41)$$

For these modes, we solve for the u_i in terms of u_5 to get

$$\frac{u_6}{u_5} = \frac{k_1^2 - k_E^2}{\varepsilon_{23}} \left(1 + \mu\Gamma \frac{\tan k_2 L}{k_2}\right)\left(\Gamma - \frac{k_M^2}{\varepsilon_{23}} \frac{\tan k_2 L}{k_2}\right)^{-1} , \qquad (42)$$

$$\frac{u_1}{u_5} = \left(k_1^2 - k_2^2\right)^{-1}\left[\left(k_2^2 - k_E^2\right) - \varepsilon_{23}\Gamma \frac{u_6}{u_5}\right] \qquad (43a)$$

$$\frac{u_2}{u_5} = \left(k_1^2 - k_2^2\right)^{-1}\left[-\mu\Gamma\left(k_2^2 - k_E^2\right) - \frac{\varepsilon_{23}}{\varepsilon_{22}} k_M^2 \frac{u_6}{u_5}\right] , \qquad (43b)$$

$$\frac{u_3}{u_5} = \left(k_1^2 - k_2^2\right)^{-1}\left[-\frac{k_1^2 - k_E^2}{\varepsilon_{23}} + \Gamma \frac{u_6}{u_5}\right] , \qquad (43c)$$

$$\frac{u_4}{u_5} = \left(k_1^2 - k_2^2\right)^{-1}\left[\mu\Gamma \frac{k_1^2 - k_E^2}{\varepsilon_{23}} + \frac{k_M^2}{\varepsilon_{22}} \frac{u_6}{u_5}\right] . \tag{43d}$$

In the limit of small ε_{23}, equations (34a, b, c) show that u_6, u_3, and u_4 all approach zero, giving a pure TE mode for which $k_1^2 \to k_E^2$.

2.5 Transverse Magnetic-like Modes

Analogously, TM-like modes are the solutions of equation (40) for which

$$\frac{k_M^2}{\Gamma\varepsilon_{22}} \frac{\tan k_2 L}{k_2} \sim 1 . \tag{44}$$

For these modes, we solve for the u_i in terms of u_6 to get

$$\frac{u_5}{u_6} = \varepsilon_{23}\left(k_2^2 - k_E^2\right)^{-1}\left[\Gamma - \frac{k_M^2}{\varepsilon_{22}} \frac{\tan k_1 L}{k_1}\right]\left[1 + \mu\Gamma \frac{\tan k_1 L}{k_1}\right]^{-1} . \tag{45}$$

Then u_i/u_6 for $1 \le i \le 4$ are given by equations (43a, b, c, d) when formally multiplied by u_5/u_6. In this case, in the limit of vanishing ε_{23}, equations (45) and (43a, b) show that u_5, u_1, and u_2 approach zero, giving a pure TM mode.

Since we consider cases for which $\varepsilon_{11} > \varepsilon_{33}$ (see discussion following eq (21a, b, c, d)), there may be solutions for which $k_M^2 > 0$, but $k_E^2 < 0$ if $\mu\varepsilon_{33}k_o^2 \le k_y^2 \le \mu\varepsilon_{11}k_o^2$. In these regions, $k_2^2 > 0$ and $k_1^2 < 0$, in which cases $k_1 = -i|k_1|$ is taken with

$$\frac{\tan k_1 L}{k_1} = \frac{\tanh\left(|k_1| L\right)}{|k_1|} . \tag{46}$$

Thus, TM-like modes may appear for thickness L where TE-like modes are below cutoff. For pure imaginary k_1, no solutions for equation (41) are possible; thus, no TE-like modes are possible for these values of k_y^2.

3. RESULTS

Calculations were performed to determine the Poynting vector, S_y, in the direction of propagation and the various field components associated with the lowest order modes. The ordinary and extraordinary indices of refraction were taken as $n_o = 2.34$ and $n_e = 2.24$, respectively, which correspond to 0.53-μm radiation ($\lambda_o = 0.53 \times 10^{-4}$ cm) in $LiNbO_3$ at 25 C. The equations scale, so that the results are identical for constant λ_o/L, where λ_o is the free space wavelength of the radiation. Several angles (θ_o) were chosen for the orientation of the dielectric axes with respect to the direction of propagation, which was kept fixed along the y-axis as shown in figure 1. The angle θ_o affects the parameters ε_{ij} according to equations (21a to d), for which $\varepsilon_1 = \varepsilon_2 = n_o^2 = 5.4756$ and $\varepsilon_3 = n_e^2 = 5.0176$.

For small angles of propagation of about $\theta_o = 5$ deg or less, the results are essentially the same as for $\theta_o = 0$ deg in which case the axes are collinear. For $\theta_o = 0$ deg, the fundamental TE and TM modes for $\lambda_o/L = 0.53$ are shown in figures 2 and 3. Although the total power flows are not normalized, one can distinguish that

a. The TE mode (fig. 2) has only one component of the E-field that is along the dielectric z-axis parallel to the surface of the slab.

b. This mode "sees" predominantly n_e, except for the energy in free space; hence, the effective index of refraction, n_{eff}, is slightly less than n_e: $n_{eff} = 2.22553$.

c. The TM mode (fig. 3) has two components of E, one perpendicular to the surface of the slab and one parallel to the surface along the direction of propagation (y).

d. This mode "sees" predominantly n_o, except for the energy in free space; hence, n_{eff} is slightly less than n_o: $n_{eff} = 2.3363$.

e. The power flow of the TE mode is closer to the surface of the slab, and a greater percentage of its energy is contained in free space. In contrast, the power flow of the TM mode is closer to the conductor.

f. The magnitude of E_y in the TM mode relative to E_x gets larger as the surface is approached from within the dielectric. (This property may be significant in understanding the interaction of these waves with SAW's.)

The modes depicted in figures 2 and 3 can be labeled the TE_o and TM_o modes in which, in general, TE_m and TM_m modes have m changes in sign in their E_z and H_z components, respectively. As L increases, the relatively little change in the form of the modes indicates that, within a fixed distance from the surface of the dielectric, there is proportionately less fractional power of the total flowing in the dielectric. For the higher order modes, m large, a larger amount of power is in the free space near the surface. As m grows larger, $n_{eff} \to 1$, $k_y^2 \to k_o^2$, and $\Gamma \to 0$; thus, the damping of the evanescent portion of the wave in free space is less severe.

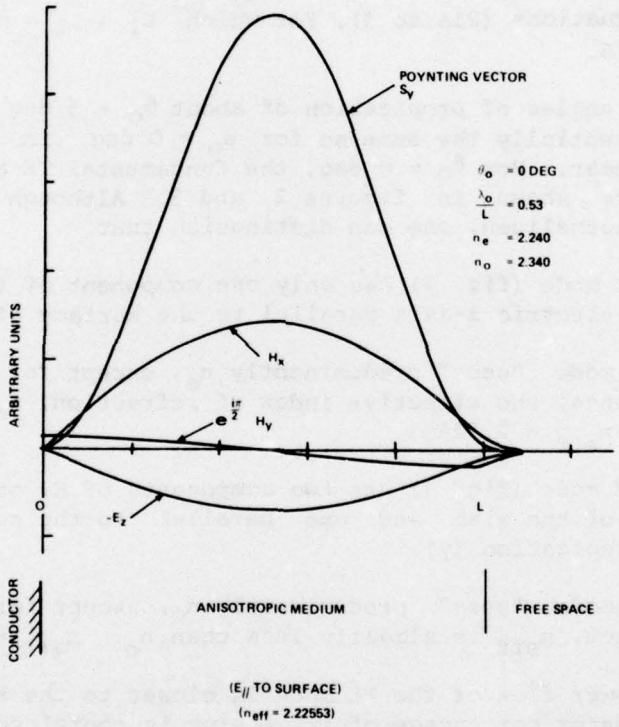

Figure 2. Electromagnetic field components for fundamental transverse electric (TE_o) mode in slab of thickness $L = \lambda_o/0.53$ for θ_0 = 0 deg angle of propagation.

The variation of n_{eff} of the TE_o mode for different L as a function of θ_o is shown in figure 4. The thickness L_m corresponds to an "m" μm thickness slab for λ_o = 0.53 μm (green) radiation; thus, the infinite medium case is rapidly approached by small thicknesses. For practical thicknesses (~1/8 in.--0.3 cm), laser radiation incident as a sheet beam over the surface of the dielectric excites a very large number of higher order modes. The variation of the field components near the surface, however, is very much like the variations near the surface depicted in figures 2 and 3.

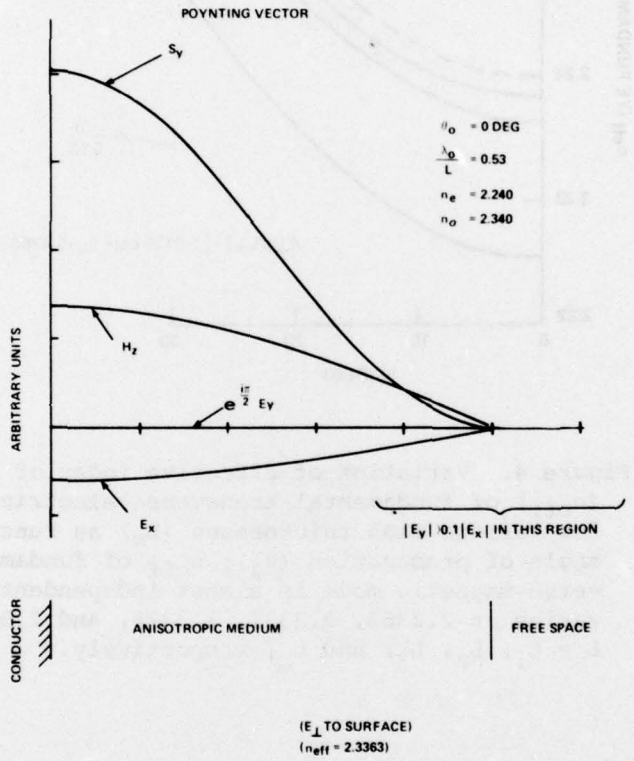

Figure 3. Electromagnetic field components for fundamental transverse magnetic (TM_o) mode in slab of thickness L = λ_o/0.53 for θ_0 = 0 deg angle of propagation.

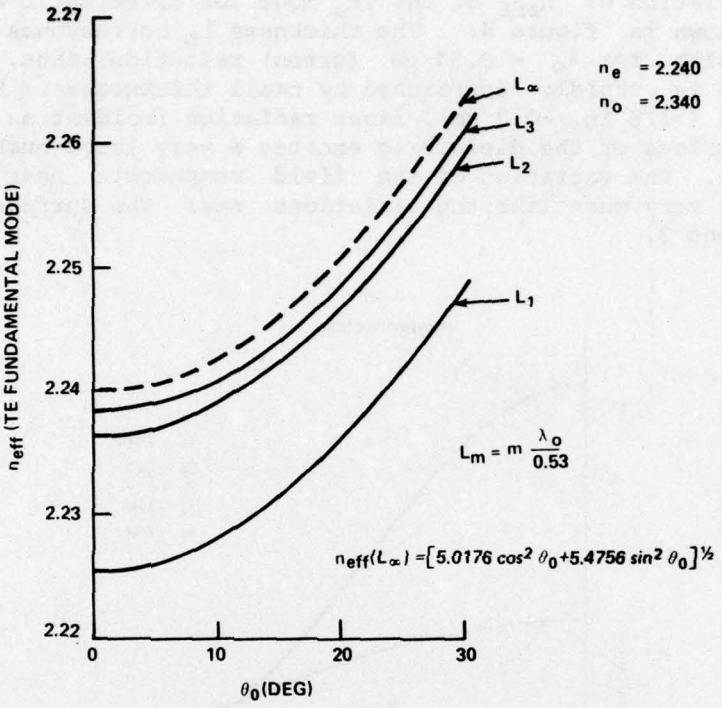

Figure 4. Variation of effective index of refraction (n_{eff}) of fundamental transverse electric (TE) mode for various slab thicknesses (L_m) as function of angle of propagation (θ_0); n_{eff} of fundamental transverse magnetic mode is almost independent of θ_0 and varies as 2.3363, 2.3391, 2.3396, and 2.340 for $L = L_1$, L_2, L_3, and L_∞, respectively.

Figure 5 shows a typical higher order mode propagating at an angle of θ_0 = 19 deg. This is a TM_2-like mode (two zero crossings for H_z), which shows the relative amounts of H_x, H_y, and E_z components generated at this angle. These components are absent in TM modes propagating at the θ_0 = 0 deg angle. The discontinuity in E_x at the surface is clearer in this higher order mode than in the TM_o mode in figure 3.

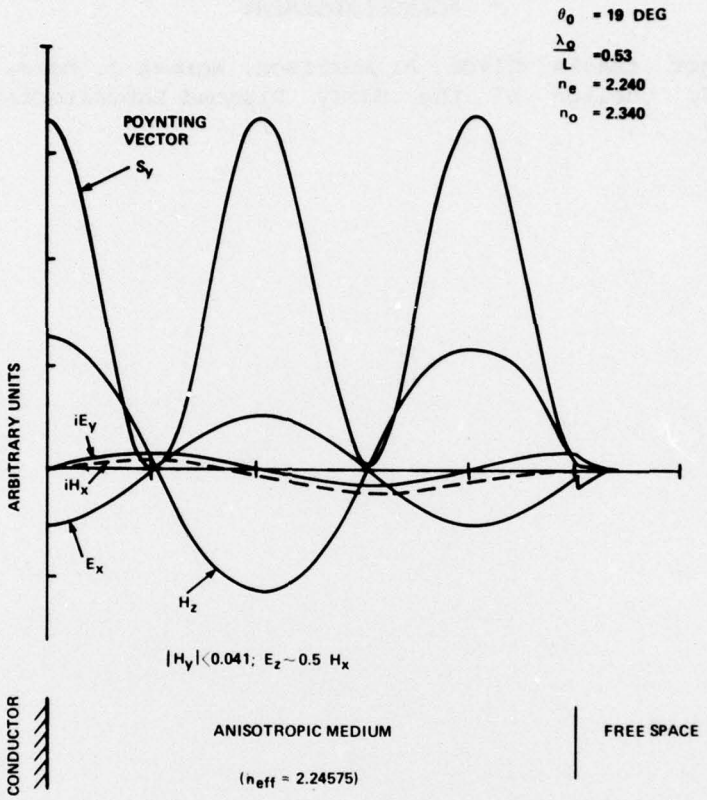

Figure 5. Electromagnetic field components for transverse magnetic (TM_2)-like mode in slab of thickness $L = \lambda_o/0.53$ for θ_0 = 19 deg angle of propagation.

4. CONCLUSIONS

These calculations show that many TE and TM modes are allowed in slabs of practical thicknesses. The problem of forming linear combinations of these modes to approximate a sheet laser beam propagating near the surfaces of thick slabs is, accordingly, formidable. What is necessary for a qualitative understanding of the interaction between such sheet beams and SAW's may be clear, however, from the examples given here. If further work is necessary for a more quantitative picture, the formalism derived here and the computer programs developed in this connection are available from the author.

ACKNOWLEDGEMENT

The author thanks Clyde A. Morrison, Norman J. Berg, John N. Lee, and Burton J. Udelson of the Harry Diamond Laboratories for helpful discussions.

DISTRIBUTION

DEFENSE DOCUMENTATION CENTER
CAMERON STATION, BUILDING 5
ALEXANDRIA, VA 22314
ATTN DDC-TCA (12 COPIES)

COMMANDER
USA RSCH & STD GP (EUR)
BOX 65
FPO NEW YORK 09510
ATTN LTC JAMES M. KENNEDY, JR.
CHIEF, PHYSICS & MATH BRANCH

COMMANDER
US ARMY MATERIEL DEVELOPMENT
& READINESS COMMAND
5001 EISENHOWER AVENUE
ALEXANDRIA, VA 22333
ATTN DRXAM-TL, HQ TECH LIBRARY
ATTN DRCDE, DIR FOR DEV & ENGR

COMMANDER
US ARMY ARMAMENT MATERIEL
READINESS COMMAND
ROCK ISLAND ARSENAL
ROCK ISLAND, IL 61299
ATTN DRSAR-ASF, FUZE & MUNITIONS
SPT DIV
ATTN DRSAR-LEP-L, TECHNICAL LIBRARY

COMMANDER
USA MISSILE & MUNITIONS
CENTER & SCHOOL
REDSTONE ARSENAL, AL 35809
ATTN ATSK-CTD-F

DIRECTOR
DEFENSE NUCLEAR AGENCY
WASHINGTON, DC 20305
ATTN APTL, TECH LIBRARY

DIRECTOR OF DEFENSE RES AND
ENGINEERING
WASHINGTON, DC 20301
ATTN TECHNICAL LIBRARY (3C128)

OFFICE, CHIEF OF RESEARCH,
DEVELOPMENT, & ACQUISITION
DEPARTMENT OF THE ARMY
WASHINGTON, DC 20310
ATTN DAMA-ARZ-A, CHIEF SCIENTIST
DR. M. E. LASSER
ATTN DAMA-ARZ-B, DR. I. R. HERSHNER

COMMANDER
US ARMY RESEARCH OFFICE (DURHAM)
PO BOX 12211
RESEARCH TRIANGLE PARK, NC 27709
ATTN DR. ROBERT J. LONTZ
ATTN DR. CHARLES BOGOSIAN

COMMANDER
ARMY MATERIALS & MECHANICS RESEARCH
CENTER
WATERTOWN, MA 02172
ATTN DRXMR-TL, TECH LIBRARY BR

COMMANDER
NATICK LABORATORIES
NATICK, MA 01762
ATTN DRXRES-RTL, TECH LIBRARY

COMMANDER
USA FOREIGN SCIENCE & TECHNOLOGY CENTER
FEDERAL OFFICE BUILDING
220 7TH STREET NE
CHARLOTTESVILLE, VA 22901
ATTN DRXST-BS, BASIC SCIENCE DIV

DIRECTOR
USA BALLISTICS RESEARCH LABORATORIES
ABERDEEN PROVING GROUND, MD 21005
ATTN DRXBR, DIRECTOR, R. EICHELBERGER
ATTN DRXBR-TB, FRANK J. ALLEN
ATTN DRXBR, TECH LIBRARY

COMMANDER
US ARMY COMMUNICATIONS RES & DEV COMMAND
FORT MONMOUTH, NJ 07703
ATTN DRSEL-GG, TECHNICAL LIBRARY
ATTN DRSEL-CT-L, B. LOUIS
ATTN DRSEL-CT-L, DR. E. SCHIEL
ATTN DRSEL-CT-L, DR. HIESLMAIR
ATTN DRSEL-CT-L, J. STROZYK
ATTN DRSEL-CT-L, DR. E. J. TEBO
ATTN DRSEL-CT-L, DR. R. G. BUSER
ATTN DRSEL-WL-S, J. CHARLTON

COMMANDER
US ARMY MOBILITY EQUIPMENT RES & DEV COMMAND
FORT BELVOIR, VA 22060
ATTN DRSEL-NV, NIGHT VISION LABORATORY
ATTN DRSEL-NV, LIBRARY

COMMANDER
USA ELECTRONICS COMMAND
WHITE SANDS MISSILE RANGE, NM 88002
ATTN DRSEL-BL, LIBRARY

DIRECTOR
DEFENSE COMMUNICATIONS ENGINEER CENTER
1860 WIEHLE AVE
RESTON, VA 22090
ATTN PETER A. VENA

COMMANDER
US ARMY MISSILE RESEARCH & DEVELOPMENT COMMAND
REDSTONE ARSENAL, AL 35809
ATTN DRDMI-TB, REDSTONE SCI INFO CENTER
ATTN DRCPM-HEL, DR. W. B. JENNINGS
ATTN DR. J. P. HALLOWES
ATTN T. HONEYCUTT

COMMANDER
EDGEWOOD ARSENAL
EDGEWOOD ARSENAL, MD 21010
ATTN SAREA-TS-L, TECH LIBRARY

COMMANDER
US ARMY ARMAMENT RES & DEV COMMAND
DOVER, NJ 07801
ATTN DRDAR-TSS, STINFO DIV

COMMANDER
WHITE SANDS MISSILE RANGE, NM 88002
ATTN DRSEL-WL-MS, ROBERT NELSON

COMMANDER
GENERAL THOMAS J. RODMAN LABORATORY
ROCK ISLAND ARSENAL
ROCK ISLAND, IL 61201
ATTN SWERR-PL, TECH LIBRARY

COMMANDER
USA CHEMICAL CENTER & SCHOOL
FORT MC CLELLAN, AL 36201

COMMANDER
NAVAL OCEAN SYSTEMS CENTER
SAN DIEGO, CA 92152
ATTN TECH LIBRARY

COMMANDER
NAVAL SURFACE WEAPONS CENTER
WHITE OAK, MD 20910
ATTN WX-40, TECHNICAL LIBRARY

DIRECTOR
NAVAL RESEARCH LABORATORY
WASHINGTON, DC 20390
ATTN CODE 2620, TECH LIBRARY BR
ATTN CODE 5554, DR. LEON ESTEROWITZ

COMMANDER
NAVAL WEAPONS CENTER
CHINA LAKE, CA 93555
ATTN CODE 753, LIBRARY DIV

COMMANDER
AF ELECTRONICS SYSTEMS DIV
L. G. HANSCOM AFB, MA 01730
ATTN TECH LIBRARY

DEPARTMENT OF COMMERCE
NATIONAL BUREAU OF STANDARDS
WASHINGTON, DC 20234
ATTN LIBRARY

DEPARTMENT OF COMMERCE
NATIONAL BUREAU OF STANDARDS
BOULDER, CO 80302
ATTN LIBRARY

NASA GODDARD SPACE FLIGHT CENTER
GREENBELT, MD 20771
ATTN CODE 252, DOC SECT, LIBRARY

NATIONAL OCEANIC & ATMOSPHERIC ADM
ENVIRONMENTAL RESEARCH LABORATORIES
BOULDER, CO 80302
ATTN LIBRARY, R-51, TECH REPORTS

DIRECTOR
ADVISORY GROUP ON ELECTRON DEVICES
201 VARICK STREET
NEW YORK, NY 10013
ATTN SECTRY, WORKING GROUP D

CRYSTAL PHYSICS LABORATORY
MASSACHUSETTS INSTITUTE OF TECHNOLOGY
CAMBRIDGE, MA 02139
ATTN DR. A. LINZ
ATTN DR. H. P. JENSSEN

HARRY DIAMOND LABORATORIES
ATTN COMMANDER/
FLYER, I.N./LANDIS, P.E./
SOMMER, H./OSWALD, R. B.
ATTN CARTER, W.W., DR., TECHNICAL
DIRECTOR/MARCUS, S.M.
ATTN WISEMAN, ROBERT S., DR., DRDEL-CT
ATTN KIMMEL, S., PAO
ATTN CHIEF, 0021
ATTN CHIEF, 0022
ATTN CHIEF, LAB 100
ATTN CHIEF, LAB 200
ATTN CHIEF, LAB 300
ATTN CHIEF, LAB 400
ATTN CHIEF, LAB 500
ATTN CHIEF, LAB 600
ATTN CHIEF, DIV 700
ATTN CHIEF, DIV 800
ATTN CHIEF, LAB 900
ATTN CHIEF, LAB 1000
ATTN RECORD COPY, BR 041
ATTN HDL LIBRARY (5 COPIES)
ATTN CHAIRMAN, EDITORIAL COMMITTEE
ATTN CHIEF, 047
ATTN TECH REPORTS, 013
ATTN PATENT LAW BRANCH, 071
ATTN GIDEP OFFICE, 741
ATTN BERG, N. J., 320
ATTN KULPA, S., 320
ATTN LEAVITT, R., 320
ATTN LEE, J. N., 320
ATTN MORRISON, C., 320
ATTN NEMARICH, J., 320
ATTN RIESSLER, W. A., 320
ATTN SATTLER, J., 320
ATTN SCHARF, W. D., 230
ATTN SIMONIS, G., 320
ATTN TOBIN, M. S., 320
ATTN UDELSON, B. J., 320
ATTN WEBER, B., 320
ATTN WILKINS, D., 320
ATTN WORCHESKY, T. L., 320
ATTN WORTMAN, D., 320
ATTN LANHAM, C., 0021
ATTN KARAYIANIS, N., 320 (10 COPIES)